



2025 Volume 51

Issue 3

Pages 152–164 https://doi.org/10.3846/gac.2025.21106

UDC 528.8.044.6

# BUILDING ALGORITHMS AND CLASSIFICATION THRESHOLDS FOR OBJECTS FROM POINT CLOUD DATA TO CREATE 3D CITY MODELS

Ngoc Quy BUI<sup>1, 4™</sup>, Anh Quan DUONG<sup>2, 4</sup>, Quoc Long NGUYEN<sup>2</sup>, Dinh Hien LE<sup>3</sup>

<sup>1</sup>Central Institute of Nature Resources and Environmental Studies, Vietnam National Unviversity, 10000 Hanoi, Vietnam <sup>2</sup>Faculty of Geomatics and Land Administration, Hanoi University of Mining and Geology, 18 Vien Street, Duc Thang, Bac Tu Liem, 10000 Hanoi, Vietnam

<sup>3</sup>Natural Resources and Environment One Member Co., Ltd, 143/85 Ha Dinh Street, Thanh Xuan, 10000 Hanoi, Vietnam <sup>4</sup>Research and Development of Geospatial Data Management and Analysis Techniques (GMA), Hanoi University of Mining and Geology, 18 Vien Street, Duc Thang, Bac Tu Liem, 10000 Hanoi, Vietnam

#### **Article History:**

- received 07 March 2024
- accepted 09 September 2025

**Abstract.** This article aims to develop an improved algorithm for classification of point cloud data. The primary component of this algorithm is determination of the classification thresholds for different geographical objects, which helps in the automatic classification of the LiDAR point cloud data. The algorithm was tested to classify the point cloud of three different areas of Ha Long city in Quang Ninh province. The results from the three areas show that for the ground points our algorithm is on average 6.4% more accurate than the traditional progressive TIN densification (PTD) algorithm. Further, with the proposed point cloud classification algorithms the average accuracy for asphalt roads is 87.77%, 98.09% for vegetation, and 96.86% for roof objects. The classified roof objects were further processed for house digitization, which provided an average accuracy of 92.07%. The whole dataset was used to develop 3D city models of the three areas (A1, A2 and A3 in Figure 7) in Hon Gai ward, Ha Long city with Level of Detail (LoD) 2.

**Keywords:** algorithms, classification thresholds, point cloud, 3D city models, Ha Long city.

### 1. Introduction

In recent years, research and development in constructing 3D city models for surface modeling and smart city construction orientation has been increased drastically. Developing a 3D city model involves integrating several different types of data such as the Digital Elevation Model (DEM), satellite images, topographic maps, digital images, and LIDAR point cloud data. The city's 3D model is highly intuitive, thereby helping managers get a better, more intuitive sense of space and the relationship between geographical entities in the area. This helps in decision making for urban management, especially smart city management with the connection of information and communication infrastructure.

One of the important inputs in high-resolution 3D city models is the LiDAR point cloud. Hence, processing and classification of the point cloud is a crucial step for constructing the 3D city models. There have been numerous articles that proposes methods and algorithms for point cloud classification to identify different objects by

classifying the point cloud into different classes. These are mainly categorised in the following two approaches: (1) algorithms based on machine learning and deep learning models, and (2) classification algorithms based on morphology and spectrum.

Machine learning and deep learning-based algorithms have been explored by various researchers for classifying point cloud data, such as, Convolutional Neuron network (Lu et al., 2020; Pujol-Miró et al., 2019; Huang et al., 2020; Boulch, 2020; Peyghambarzadeh et al., 2020; Wen Chenglu et al., 2019; Wen Congcong et al., 2020), Active learning (Weidner et al., 2020), Random Forest (Weidner et al., 2019; Park & Guldmann, 2019), Multiview Sematic Learning network (Yang et al., 2020a), and Atrous XCRF's algorithm (Arief et al., 2019). With the development of modern computing systems and cloud computing, deep learning algorithms have become the new standard for processing big data, including point clouds.

Morphological and spectral classification algorithms are popularly used in point cloud data classification applications serving the fields of geography and geology. A

<sup>&</sup>lt;sup>™</sup>Corresponding author. E-mail: quybncres@vnu.edu.vn

few of these methods are morphological application combined with fuzzy logic (Rastiveis et al., 2020), morphological focus network algorithm (Li et al., 2020), and combining shapes-morphology-texture in geomorphological classification (Guo et al., 2019). Along with the above studies, there are structure-based algorithms (Hamid-Lakzaeian, 2019; Xue et al., 2019; Huang et al., 2018) or based on 3-dimensional characterization of data (Yang et al., 2020b; Williams & Ilieş, 2018; Stojanovic et al., 2019). Besides, super voxel classification algorithms are also applied in studies on point cloud classification (Lin et al., 2018; Kang & Yang, 2018; Zhu et al., 2017). One of the most widely used algorithms that use spectral classifier is hyperspectral (Gerke & Xiao, 2014; Brell et al., 2019; Suomalainen et al., 2011) or feedback signal analysis (Tseng et al., 2015; Lai et al., 2019).

In particular, surveying and mapping technology has made significant progress with many advanced technologies such as unmanned aerial vehicles (UAV), ground laser scanning systems, aviation laser scanning systems, GNSS systems, etc. The current data collection measurement technology has gradually shifted from traditional measuring devices, single point to point, to devices that collect spatial information comprehensively and speedily, such as ground laser scanners, mobile laser scanners (mobile mapping), and LiDAR scanners on aircraft or UAVs. The standard data format for these devices is 3D point cloud data that carry accurate information about geographic coordinates and much other information such as color, reflection intensity, and pulse feedback. With the advent of 3D point cloud data, the real world can be entirely presented at the true scale. Moreover, the increasing volume of collected 3D point cloud data has facilitated the provision of diverse and complete information sources for classifying and constructing objects useful in developing 3D city models. The developed 3D city models can be augmented with different levels of detail (LoD0 to LoD4), which are the attribute information that serves various applications, such as, Urban design and management; Spatial planning; Identification of environmental issues, and urban environmental management; Disaster prevention and response to situations; Application in Tourism & heritage conservation.

Therefore, the point cloud classification will provide an input source for building 3D city models. However, with the large volume of data, the classification of point cloud data is mainly based on the tools of the accompanying commercial software of the data collection equipment manufacturers. Therefore, the construction of an automatic point cloud classification technology process to serve the establishment of 3D city models based on researching and building algorithms and programs to classify different objects of data automatically is required. Hence, in this study, we have presented a set of algorithms, which helps in the automatic classification of point cloud data. These are explained in detail in the next section.

#### 2. Methods

This section describes the algorithms used in this study for point cloud classification. These algorithms are integrated to automatically classify the point cloud into eight different classes and subclasses, excluding water. A broad description of feature classes and thresholds used in the algorithms are depicted in Figure 1 and are described in consecutive sections.

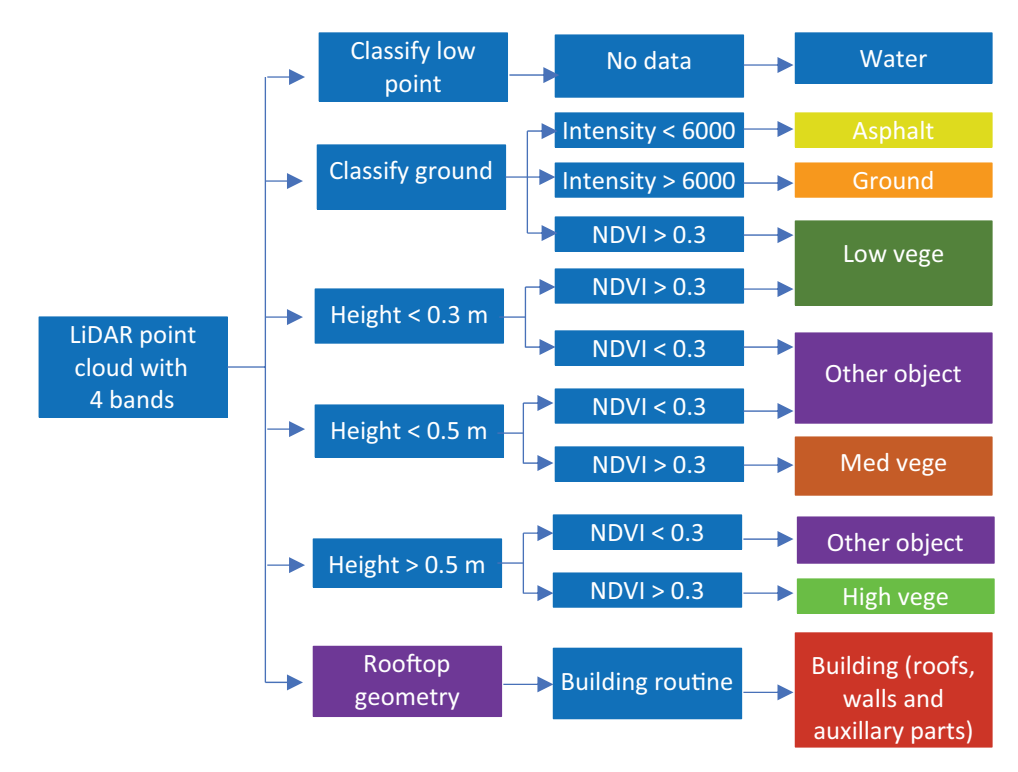


Figure 1. The threshold for classifying objects from point cloud data (modified from Bui et al., 2021)

### 2.1. Noise filtering algorithm

Noise points are inevitable in LiDAR scanning, primarily, due to the presence of low clouds, suspended particles, flying birds, and objects suspended on the water surface or noise points can also be due to simply the error in the scanned data. However, in the modern LiDAR scanning systems, these noise points are often automatically filtered out. This is because of the use of an algorithm that determines the difference between two scan sessions, which filters out the points of the exact location that only appear in the first scan but not in the second scan. However, despite this advancement, the noise points may still be present due to a multitude of reasons. Therefore, the noise filtering algorithm must still be used to filter out these points. In this study, the following two criteria are used for noise filtering of the LiDAR point cloud: 1) the score is lower than the surrounding points, and 2) the isolated standing points.

The score lower than the surrounding points criterion will look for points with a limited number of points and are lower in elevation than most of the surrounding points (Figure 2). When removed, these single-standing low points will create favorable conditions for accurately determining the land surface by the ground algorithm proposed in the research. This algorithm will start from the lowest points because the lowest points will always be on the ground unless these points are error measurement points.

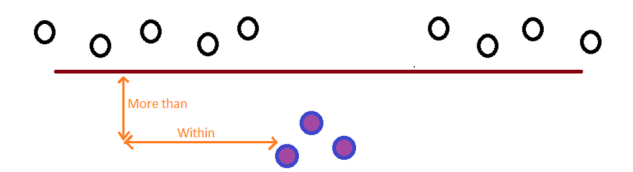


Figure 2. The low point algorithm

The isolated standing point criterion will help identify and filter out clusters of points that are far apart from neighboring points. These isolated and suspended points, if not interference points, are also the points that are not needed.

Further, automatic digitizing algorithms are also used for zoning the areas where no data is available, e.g., hydrological regions due to zero reflectance of LiDAR rays.

### 2.2. Ground filter algorithm

In this paper, the progressive TIN densification (PTD) algorithm has been used for enhanced separation of ground and non-ground points in a point cloud. The method includes two implementations of the ascending triangle network distribution algorithm, the first time with the smaller parameter values, and at the same time, will limit the distribution of extra points when the side of the triangle is smaller than a given parameter. After the first distribution reaches this limit, the first search will stop, and the found ground points will be used as starting points for

the second search with other search parameters suitable for finding all details on the ground. The starting point for the first search is the lowest in a given square. This square will be smaller than the size of the largest house in the area to avoid misidentifying the starting point located on the roof. Due to the selection of the lowest point to return to the ground, the error points need to be eliminated by the noise filtering algorithm in advance. This approach is sometimes also known as the iterative PTD algorithm.

The improved PTD ascending triangular network distribution method proposed in the paper is described in Figure 3, and the enhanced ground point filtering algorithm is shown in Figure 4.

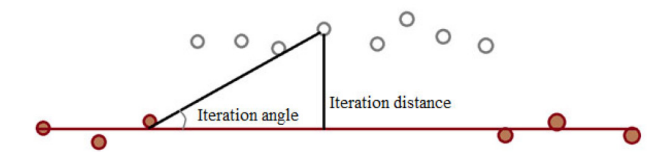


Figure 3. The ground filter algorithm

In this two step PTD algorithm, the first step works on the complete LiDAR point cloud (noise-filtered) and includes the following steps:

- Step 1: Enter the parameter values. Includes 4 parameters that need to be determined as follows: Maximum house size determines the maximum size of the search grid; iteration angle is the maximum angle between the TIN face and the line linking an unclassified point to the nearest vertex of that face; iteration distance is the maximum distance from an unclassified point to the corresponding TIN face, these two values are illustrated in Figure 2; edge length value to stop the point distribution (side length represents the minimum threshold for the largest side length of the triangle).
- Step 2: Choose a starting point. This is the lowest point in a range larger than the maximum house size parameter. Therefore, filtering for points lower than the soil surface needs to be done in advance. This starting point will be selected to find the first TIN triangle, starting a continuous loop that automatically finds other ground points.
- Step 3: Point distribution loop. The loop will continuously find ground points that satisfy the 3 parameter values of iteration angle, iteration distance, and edge length from the original point layer. The loop will end when no more satisfying points can be found. In the first round of PTD filtering, the edge length parameter will be used to stop the point distribution to help find the most reliable ground points with a large edge length value.

The result of the first filter round will be a layer of ground points with a density equal to the large edge length value to stop the point distribution. This layer of ground points will be used as the starting point for the second round of PTD filtering including the following steps:

- Step 1: Enter the parameter values. Includes 2 parameters that need to be determined as follows: the iteration angle and the iteration distance have a different value from the value of the first search loop.
- Step 2: Choose a starting point. Use all the ground points generated from the first filter as the starting point.
- Step 3: Point distribution loop. The loop will continuously find the ground points that satisfy the 2 parameter values of iteration angle, the iteration distance is set. The loop will end when no more satisfying points can be found.

The result of this second filtering process will help find all ground points. This ground classification approach is implemented using the built-in ground classification algorithm.

# 2.3. Algorithm for classifying the points of asphalt road

Table 1 lists the LiDAR reflectance of various features as provided by Riegl, the LiDAR instruments manufacturer.

From Table 1, it is observed that the intensity value of the LiDAR point cloud can be used to separate various

objects, especially when there is a large difference between reflectances.

The asphalt classification algorithm proposed in this article uses the intensity value of the point cloud to separate the asphalt layer from the ground layer. It can be seen from Table 1 that the asphalt layer has a very low reflectivity, which is different from the rest of the ground objects.

The intensity value of the point cloud from the City-Mapper is stored in 16-bit format, thus the value from weak to strong varies from 0–65535. After multiple test processings, an intensity threshold of 6000 is selected that separates asphalt from other ground points with the highest quality. Due to the light absorbing characteristic, asphalt has the lowest intensity value as compared with other materials in the study areas. There are some exceptions, however, those abnormal points mostly stand separately and in a small number. Therefore, those points are filtered back to the ground layer with the isolated standing point algorithm.

The asphalt classification algorithm is implemented on the ground layer (obtained after enhanced PTD classification), which results in two layers: asphalt road point clouds and remaining ground point clouds.

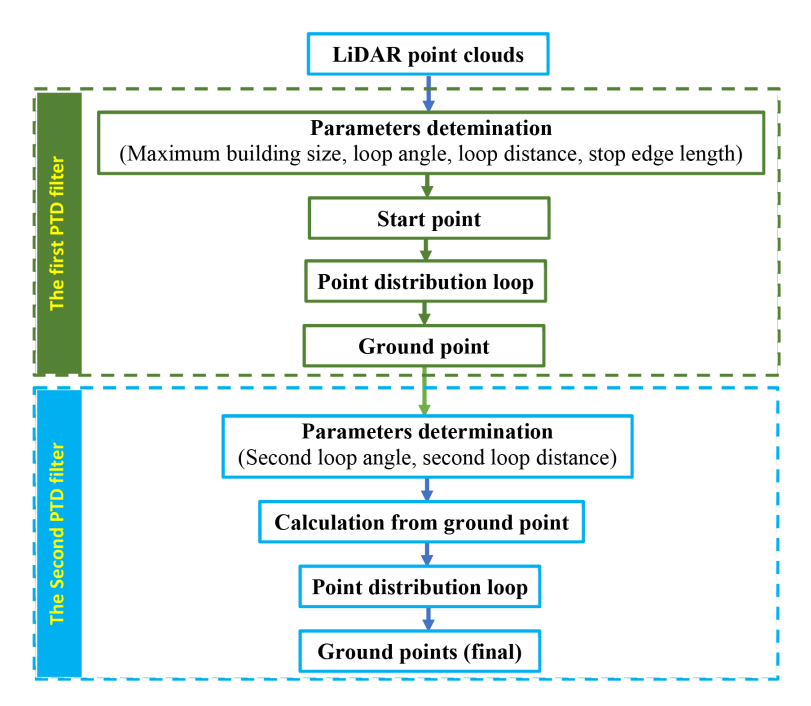


Figure 4. The enhanced ground point filtering algorithm

**Table 1.** Response intensity of different surface types

Material	Reflectance (%)	Material	Reflectance (%)
White paper	Up to 100	Carbonate sand (dry)	57
Flat wood material	94	Beach sand	50
Snow	80–90	Carbonate sand (wet)	41
Sponges	88	Conifer	30
White clay	85	Fine concrete	24
Granit and clay	Up to 75	Asphalt and pebble stones	17
Newspaper	69	Lava	8
Tissue	60	Black rubber	2

### 2.4. Vegetation classification algorithm

The normalized difference vegetation index (NDVI) is used for classifying the vegetation in the point cloud. NDVI values (from multi-spectral images) for each point in the point cloud are combined with the corresponding elevation values to classify the vegetation layer. NDVI value helps in avoiding misclassification of buildings and other non-vegetation points into the vegetation class. The altitude classification algorithm used in the paper is shown in Figure 5.

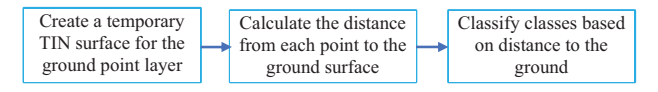


Figure 5. Algorithm for classification by altitude

A TIN based bare earth model is generated using the ground points. Then the elevation of all the non-ground points is measured with respect to this bare earth model. A combination of the NDVI and elevation of the points are used to categorize the point cloud into three classes:

- Low vegetation (grasses, vegetables, crops): elevation 0–0.3 m and NDVI > 0.3;
- Medium vegetation (ornamental plants, shrubs, etc): elevation 0.3–0.5 m and NDVI > 0.3; and
- High vegetation (trees and urban greenery): elevation >0.5 m and NDVI > 0.3.

NDVI value of 0.3 was selected because it provided the highest accuracy after several tests runs in three study areas.

### 2.5. Roof filtering algorithm

The roof filtering algorithm uses the plane-expansion clustering method with other algorithms to classify the house point classes, i.e., roofs and walls. The flowchart of this algorithm is shown in Figure 6.

The point cloud obtained after separating ground and vegetation points is used as input in this algorithm. These remaining feature points that are higher than the ground level, are not vegetation, and have the shape of flat surfaces are likely to belong to the structures identified built by humans. Therefore, the primary step of this algorithm is to cluster the planes on this remaining point cloud.

Further, the following two parameters are attached to the plane clusters to assure that the clustered plane points are roof objects:

- Minimum size of the roof: helps distinguish the house roof from objects such as vehicles, trash cans, mailboxes, etc., because these also have a flat surface but are smaller in size.
- Surface thickness: determines the thickness of clustered plane points to accept it as a roof. This parameter is based on the noise of the point cloud, the convexity, and the patterns of the roof surfaces.

Another important parameter in this algorithm is the slope angle of clusters. The clusters with a slope angle from 88°–90° will belong to the objects such as house

walls or billboards. Therefore, plane point clusters having a slope less than 88° are selected to identify the house roof point layer. Within and near this roof layer that contains flat surfaces, other roof details or auxiliary parts such as chimneys and musty (stair covers on the roofs) are identified from the point cloud using a distance threshold. Subsequently, the point cloud under the roof layer is classified as the wall layer. The roof, auxiliary parts, and the wall point clouds, together form the house point cloud layer. These layers are an important input to automatically digitize and build 3D models of the house blocks.

After all the aforementioned point cloud classifications, the remaining point cloud data is treated as other feature classes.

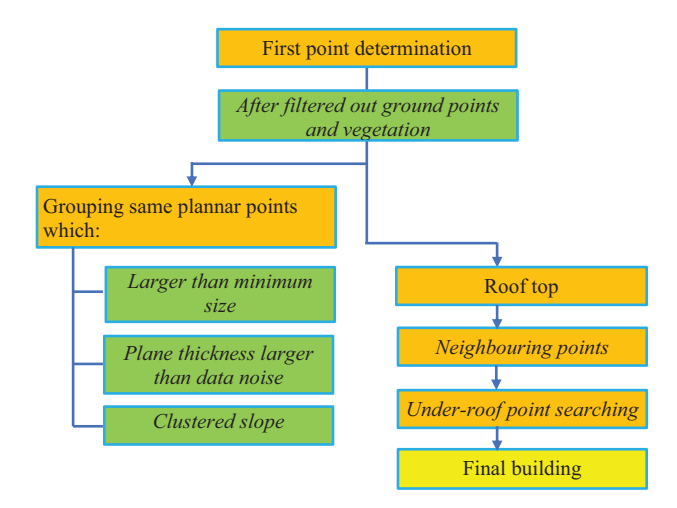


Figure 6. Roof filter algorithm

### 3. Experiment and analysis

### 3.1. Experiment location and data

The LiDAR point cloud classification algorithms discussed above are implemented in three study areas based on three different housing characteristics in Hon Gai, Ha Long city, Quang Ninh province (Figure 7). The first area has an area of 27.6 hectares in Hong Hai ward, which is a newly built urban area and includes several villas and townhouses, schools, and sports fields. The second area is an ancient urban area in Bach Dang ward having an area of 27.3 hectares. This area has a very dense density of houses, mainly houses that were built a long time ago, and at the same time has an additional area with plants providing food. The third area is the latest construction area with many high-rise buildings along with the newly opened coastal road, including parks, squares, and some administrative buildings of the city. This area belongs to the Hong Gai ward, with an area of 29.5 hectares.

### 3.2. Accuracy evaluation

The article uses the accuracy assessment method used by Cai et al. (2018) to evaluate their process of automatic digitization of objects from remote sensing images. This



Figure 7. Assessment areas in Ha Long city: A1 - Hong Hai; A2 - Bach Dang; A3 - Hong Gai

accuracy assessment method includes five components:
1) object match assessment; 2) accurate range assessment;
3) quantity-based assessment; 4) similarity-based assessment and 5) distance-based assessment. However, for the present study, only two of the above five and an additional method need to be used: 1) to evaluate the object match, 2) to evaluate the accuracy range, and 3) to evaluate the numerical accuracy.

Object match assessment is done by comparing the area of the digitized object with respect to the reference object. The overall fit index  $(O_{ij})$  value for the comparison of the two objects is given by

$$Q_{ij} = \frac{1}{2} \left( \frac{A_{C,i} \cap A_{R,j}}{A_{C,i}} + \frac{A_{C,i} \cap A_{R,j}}{A_{R,j}} \right), \tag{1}$$

where  $A_{R,j}$  is the total area value of the reference objects,  $A_{C,i}$  is the value of the total area of the evaluated/digitized object, and  $A_{C,i} \cap A_{R,j}$  is the interference area.  $O_{ij}$  helps show the evaluated object's match compared to the referenced object.

The second evaluation method is the area-based assessment method. This method helps to evaluate the level

of accuracy and completeness based on the two equations below:

$$P_{AC} = \frac{A_C}{A_{DC}}; (2)$$

$$P_{AR} = \frac{A_C}{A_{RC}},\tag{3}$$

where  $P_{AC}$  accuracy is the ratio of the area of the automatically classified area ( $A_C$ ) to the total area of the automatically classified area ( $A_{DC}$ ). The  $P_{AC}$  accuracy will range from 0 to 1; if all objects are classified correctly, then  $P_{AC}=1$ .  $P_{AR}$  is the completion level and is given as the ratio of  $A_C$  to the total area of the reference area ( $A_{RC}$ ). The  $P_{AR}$  completeness will range from 0 to 1. If all the auto-classified objects exactly match the reference area, then  $P_{AR}=1$ .

The third evaluation method is the quantitative method. This method helps to evaluate the level of accuracy and completeness based on the following two equations:

$$P_{NC} = \frac{N_C}{N_{DC}}; (4)$$

$$P_{NR} = \frac{N_C}{N_{RC}},\tag{5}$$

where  $P_{NC}$  accuracy is the ratio of the number of objects automatically classified correctly  $(N_C)$  to the total number of objects classified  $(N_{DC})$ . The  $P_{NC}$  accuracy will range from 0 to 1. If all objects are automatically classified correctly, then  $P_{NC}=1$ .  $P_{NR}$  completeness is the ratio of  $(N_C)$  to the total number of objects in the reference data  $(N_{RC})$ . The  $P_{NR}$  completeness will range from 0 to 1. If all the auto-classified objects exactly match the reference objects, then  $P_{NR}=1$ .

### 4. Results and discussion

# 4.1. Evaluation of the accuracy of the ground point classification algorithm

Area-based accuracy assessment is used to evaluate the accuracy of the used automatic ground filtering algorithm. The enhanced ground classification algorithm is implemented on the built-in software, and the results are also compared with the traditional PTD method implemented on TerraSolid software.

The classified ground points are checked manually using different views and ways of displaying them in TerraSolid prior to calculating the statistics in the area. For the three areas together, the total number of ground points identified with the traditional PTD algorithm is 675 000 points, and with the improved PTD 1244000 points.

In Figures 8a, and 8b, the orange points are the ground points that have been correctly classified, and the blue points are the points that are the ground but have not been classified by the algorithm.

The total reference area of study area A1 is  $A_{RC} = 179~690~\text{m}^2$ . For the traditional PTD method, after manual testing and statistics: the area that is automatically classified is  $A_{DC} = 176~044~\text{m}^2$  and the automatically correctly classified area is  $A_C = 161~380~\text{m}^2$ . For the improved PTD method, the total automatically classified area is  $A_{DC} = 178~529~\text{m}^2$  and the correctly classified area is  $A_C = 174~030~\text{m}^2$ . Finding the similar values for study areas A2 and A3,  $P_{AC}$ , and  $P_{AR}$  for all three study areas are calculated and shown in Table 2.

**Table 2.** Results of comparing the accuracy and completeness of the proposed ground filter algorithm with that of the classical PTD algorithm

	$P_{AC}$		$P_{AR}$	
Areas	Classical PTD	Enchanced PTD	Classical PTD	Enchanced PTD
A1	0.9167	0.9748	0.8981	0.9685
A2	0.8832	0.9515	0.8656	0.9493
A3	0.9017	0.9668	0.9149	0.9763

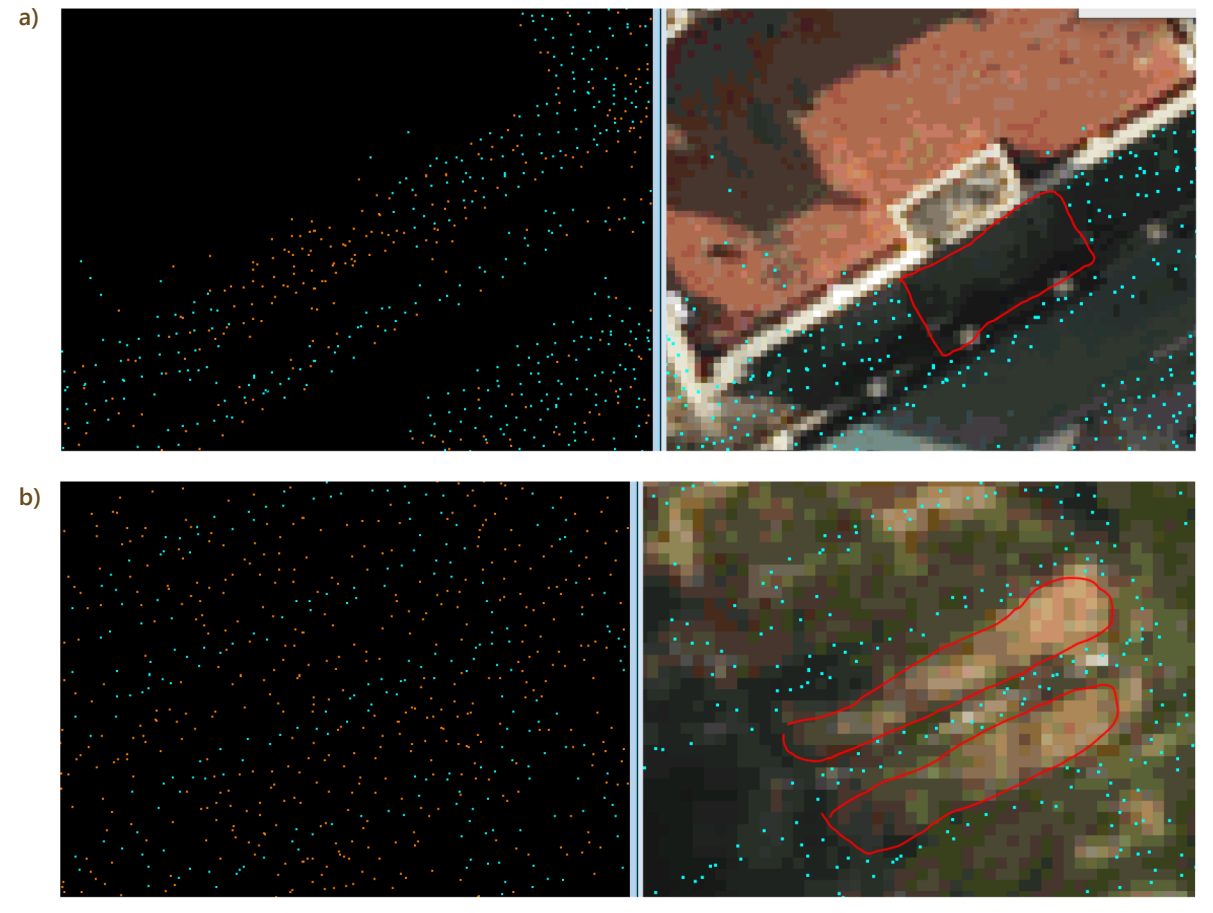


Figure 8. Inaccurate ground filter area statistics: a) a part of the image was derived from data of the A1 – Hong Hai area; b) a part of the image was derived from data of the A2 – Bach Dang area

From the experimental results, it can be seen that the enhanced PTD ground classification algorithm has higher accuracy than the traditional PTD ground classification algorithm, which helps to reduce manual effort while saving time and human resources.

# 4.2. Evaluation of point cloud automatic classification accuracy

The process of automatic point cloud classification is performed according to the proposed algorithm based on the designed software of the article. The accuracy assessment for all classified classes is performed by a manual inspection using multidimensional views of point cloud data in TerraSolid. The ortho images are used as the reference data.

## 4.2.1. Assessment of asphalt automatic classification accuracy

In Figure 9, areas with red contours mark the size of the entire area classified as asphalt. The gray point layer depicts the correctly classified asphalt point while yellow points are the incorrectly graded asphalt point. The blue outlines mark the actual asphalt area. The automatic road classification algorithm is assessed using  $P_{AR}$  and  $P_{AC}$ .

The total reference area of asphalt road in study area A1 is  $A_{RC} = 45760 \text{ m}^2$ , the total automatically classified asphalt road area is  $A_{DC} = 49119 \text{ m}^2$  and the correctly classified asphalt road area is  $A_C = 45403 \text{ m}^2$ . Finding the similar values for study areas A2 and A3,  $P_{AC}$ , and  $P_{AR}$  for all the three study areas are calculated and shown in Table 3.

Repeat the assessment with sites A2 and A3, the result is shown in the following table:

**Table 3.** Results of the accuracy of an asphalt classification algorithm for 3 study areas

Asphalt	P <sub>AC</sub>	$P_{AR}$	
A1	0.9243	0.9922	
A2	0.8815	0.9139	
A3	0.8273	0.8592	

The accuracy and completion achieved from the asphalt road classification algorithm varies up to 10% in the

three study areas. The variation in the results is because some yard tiles also have low reflectivity, similar to the reflective level of asphalt. Additionally, the range of intensity values of asphalt in an area also has a significant variation. Therefore, the level of completion can be increased by increasing the search parameters, however, accuracy may get reduced due to the false detection of other objects. Only A1 has considerable uniformity in the intensity values of asphalt, hence, the classification algorithm provides the best results in this area.

## 4.2.2. Evaluate the accuracy of automatic classification of plant objects

In Figure 10, the green points are the tree points that have been automatically correctly classified points. Purple points are those, which are automatically classified but give false results. The pink points are unclassified plant points. The automatic plant classification algorithm is assessed using  $P_{NC}$  and  $P_{NR}$ .

The total reference points belonging to the plant objects in study area A1 is  $N_{RC}$  = 2013402, the total automatically classified plant points is  $N_{DC}$  = 2020698 and correctly classified plant points  $N_{C}$  = 2001080. Finding the similar values for study areas A2 and A3,  $P_{NC}$  and  $P_{NR}$  for all the three study areas are calculated and shown in Table 4.

**Table 4.** Results of the accuracy of plant classification algorithms for 3 study areas

Plant	P <sub>NC</sub>	P <sub>NR</sub>	
A1	0.9903	0.9939	
A2	0.9718	0.9691	
A3	0.9806	0.9869	

From Table 4, it is observed that the accuracy and completion of the plant classification algorithm are relatively high and consistent in all the three study areas. The average accuracy of the algorithm is 98.09%, and the average completion at the level of 98.33% is achieved. The reason for these high values can be due to one, more, or all of the following reasons: (1) combining elevation with NDVI values, (2) the plant objects in the areas are quite uniform in species, and (3) there is less temporal variation in data





Figure 9. Statistics of classification results of asphalt roads

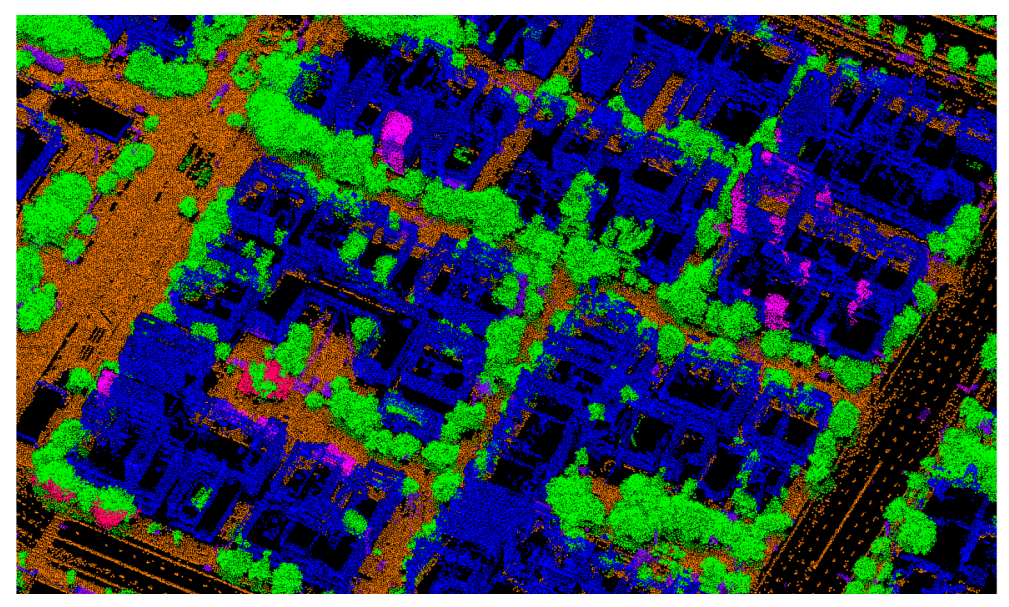


Figure 10. High plant classification algorithm results

collection of the three study areas, hence, almost all plants have green foliage that further enhanced the use of NDVI. The misclassified plant points mainly belong to the rooftop and hanging (from the wall) plants.

## 4.2.3. Assess the accuracy of automatic home classification

In Figure 11, the red points are the roof points that have been automatically correctly classified points. Blue points are those, which are automatically classified but give false results. The automatic plant classification algorithm is assessed using  $P_{AC}$  and  $P_{AR}$ .

The total reference area of roofs in study area A1 is  $A_{RC} = 102822 \text{ m}^2$ , the total automatically classified roof area is  $A_{DC} = 103526 \text{ m}^2$  and the correctly classified roof area is  $A_{C} = 101970 \text{ m}^2$ . Finding the similar values for study areas A2 and A3,  $P_{AC}$ , and  $P_{AR}$  for all the three study areas are calculated and shown in Table 5.

**Table 5.** Results of the accuracy of roof classification algorithm for 3 study areas

Building	Accuracy	Completion level
A1	0.9850	0.9917
A2	0.9518	0.9676
A3	0.9691	0.9557

From Table 5, it is observed that the accuracy and completion of the roof classification algorithm is also high and consistent in all the three study areas. The average accuracy of the algorithm is 96.86%, and the average completion at the level of 97.17% is achieved depicting that most of the roof area is correctly classified. Study area A1 has the highest accuracy and completeness due to similarity in the house architecture in this area. Study area A2 has the lowest accuracy because this area has a high house

density and moreover, the houses have distinctive features as these were built decades ago. There are a few areas that are misclassified as roof points. These are primarily sunshades or bus shelters, which are sometimes similar to house roofs. Also, due to the low height and large width, unclassified roofs are mistakenly classified as ground objects, but these false cases account for a small percentage.

## 4.2.4. Evaluate the accuracy of the house automation algorithm

The regional house digitization file is used as the collation data to evaluate the accuracy of the automatic house digitization algorithm (Figure 12) using  $O_{ij}$  object-fit,  $P_{AC}$  area accuracy, and  $P_{AR}$  area completeness, given in Section 3.

The accuracy assessment results of the home digitization algorithm for the three study areas are shown in Table 6.

**Table 6.** Matching, accuracy results of home digitization algorithm for three evaluation areas

House digitization	Matching degree	Accuracy	Completion level
A1	0.9285	0.9450	0.9371
A2	0.9217	0.9288	0.9362
А3	0.9118	0.9331	0.9217

The above results show that the accuracy of the house digitization algorithm is smaller than the accuracy of the house classification algorithm. This is understandable because the houses are automatically digitized on the classified roof layer data. Therefore, the house classification algorithm's accuracy directly affects the home digitization algorithm's accuracy.

From Table 6, it can be seen that the accuracy of the house automation algorithm proposed in the article is relatively high, with the object matching values and the

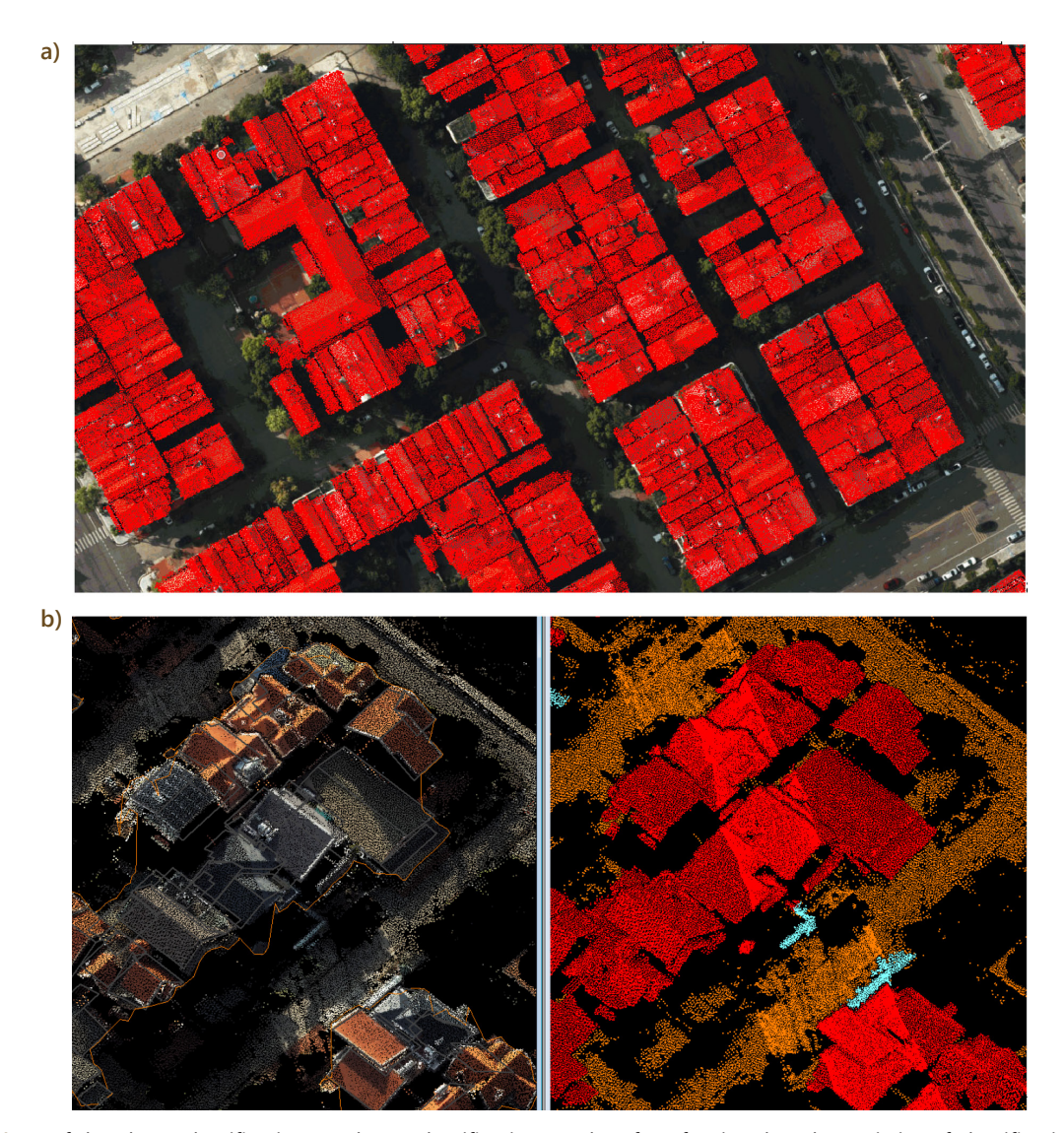


Figure 11. Roof data layer classification results: a) classification results of roof point class; b) statistics of classification results of roof point class

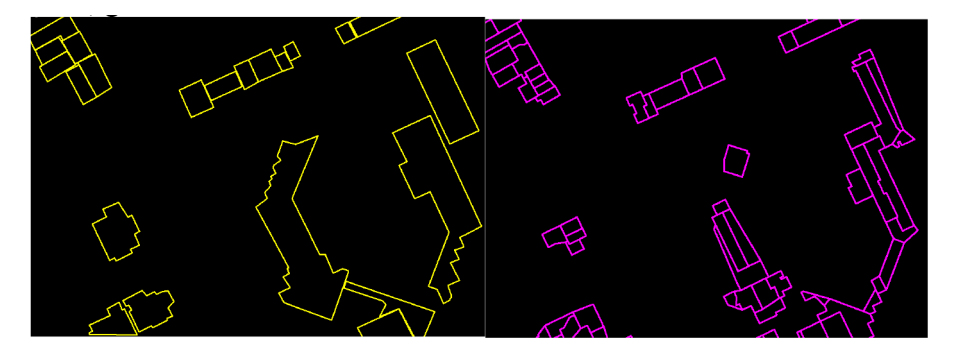


Figure 12. Reference data (left) and home automation results (right) of the assessment area

accuracy of all three sites being greater than 0.9; the level of the completion of the three sites is as follows: 0.9371–0.9362–0.9217, showing that the algorithm has digitized most of the houses. The houses that are missing or incorrectly digitized are mainly due to the complex and/or heterogeneous roof structures, and roofs covered

with vegetation. Besides, with the match and completion results above 0.9, it shows the high automation ability of the algorithm, helping to reduce manual effort. Considering each area separately, it can be seen that A1 has a uniform square house, so it has better automatic digitization results than A2 and A3.



Figure 13. 3D city model of Hon Gai, Ha Long, Quang Ninh province: a) a part of the 3D model of A1 – Hong Hai area; b) a part of the 3D model of A2 – Bach Dang area; c) a part of the 3D model of area A3 – Hong Gai area

# 4.3. Results of building 3D city models in Hon Gai, Ha Long, Quang Ninh province

With the 3D terrain background, an image map, and content objects processed and classified according to the proposed process, including vegetation, roads, hydrological systems, buildings, and other geographical features, the 3D city model of Hon Gai area in Ha Long city, Quang Ninh province, have been constructed (Figure 13).

The developed 3D city model can reach the Level of Detail 2 (LoD2) and hence, can be used for many different purposes such as Security – Defense; Urban design and management, Spatial planning, Identification of environmental issues and urban environmental management, Disaster management and mitigation, Application in Tourism & heritage conservation, etc.

### 5. Conclusions

The article has built a set of automatic point cloud classification algorithms based on researching and synthesizing existing point cloud classification algorithms and studying the characteristics of LiDAR point cloud data. Newly re-

leased into eight different subclasses, with high accuracy. With the proposed algorithm, we can completely build automatic point cloud classification software, which will be a tool to help improve efficiency and production efficiency for point cloud data classification. While in Vietnam, studies on point cloud classification algorithms are limited, mainly focusing on ground point classification, and most manufacturing units use available algorithms of commercial software.

The experimental implementation of the point cloud classification algorithm and the automatic process of building 3D city models at Hon Gai experimental area, Ha Long city, has demonstrated the ability to deploy real data by the set of algorithms and the automatic process of building 3D city models. The evaluation results in three sites of the experimental area show that the set of algorithms brings automation and high accuracy, and the 3D city model is built automatically, which saves costs and production time. This indicates that the set of point cloud classification algorithms, the threshold of classification criteria, and the automatic process of building 3D city models proposed in the article are highly automated, helping to improve the efficiency of data production of the

existing data at enterprises, contributing to increasing the speed and reducing the cost of data production, creating favorable conditions for developing more modern and advanced applications.

### **Acknowledgements**

This paper is funded through the project by the Ministry of Education and Training Science project (N0. B2021-MDA-01), Vietnam. The authors would like to thank Dr. Ropesh Goyal from IIT Kanpur for providing comments and editing this manuscript.

### References

- Arief, H. A., Indahl, U. G., Strand, G. H., & Tveite, H. (2019). Addressing overfitting on point cloud classification using Atrous XCRF. ISPRS Journal of Photogrammetry and Remote Sensing, 155, 90–101. https://doi.org/10.1016/j.isprsjprs.2019.07.002
- Boulch, A. (2020). ConvPoint: Continuous convolutions for point cloud processing. *Computers & Graphics*, 88, 24–34. https://doi.org/10.1016/j.cag.2020.02.005
- Brell, M., Segl, K., Guanter, L., & Bookhagen, B. (2019). 3D hyper-spectral point cloud generation: Fusing airborne laser scanning and hyperspectral imaging sensors for improved object-based information extraction. *ISPRS Journal of Photogrammetry and Remote Sensing*, 149, 200–214.
  - https://doi.org/10.1016/j.isprsjprs.2019.01.022
- Bui, N. Q., Le, D. H., Duong, A. Q., & Nguyen, Q. L. (2021). Rule-based classification of airborne laser scanner data for automatic extraction of 3D objects in the urban area. *Journal of the Polish Mineral Engineering Society*, 1(2), 103–114. https://doi.org/10.29227/IM-2021-02-09
- Cai, L., Shi, W., Miao, Z., & Hao, M. (2018). Accuracy assessment measures for object extraction from remote sensing images. *Remote Sensing 10*(2), Article 303. https://doi.org/10.3390/rs10020303
- Gerke, M., & Xiao, J. (2014). Fusion of airborne laserscanning point clouds and images for supervised and unsupervised scene classification. *ISPRS Journal of Photogrammetry and Remote Sensing*, 87, 78–92. https://doi.org/10.1016/j.isprsjprs.2013.10.011
- Guo, J., Liu, Y., Wu, L., Liu, S., Yang, T., Zhu, W., & Zhang, Z. (2019). A geometry- and texture-based automatic discontinuity trace extraction method for rock mass point cloud. *International Journal of Rock Mechanics and Mining Sciences*, 124, Article 104132. https://doi.org/10.1016/j.ijrmms.2019.104132
- Hamid-Lakzaeian, F. (2019). Structural-based point cloud segmentation of highly ornate building façades for computational modelling. *Automation in Construction*, *108*, Article 102892. https://doi.org/10.1016/j.autcon.2019.102892
- Huang, R., Xu, Y., Hong, D., Yao, W., Ghamisi, P., & Stilla, U. (2020). Deep point embedding for urban classification using ALS point clouds: A new perspective from local to global. *ISPRS Journal of Photogrammetry and Remote Sensing*, 163, 62–81. https://doi.org/10.1016/j.isprsjprs.2020.02.020
- Huang, R., Yang, B., Liang, F., Dai, W., Li, J., Tian, M., & Xu, W. (2018). A top-down strategy for buildings extraction from complex urban scenes using airborne LiDAR point clouds. *Infrared Physics and Technology*, 92, 203–218. https://doi.org/10.1016/j.infrared.2018.05.021
- Kang, Z., & Yang, J. (2018). A probabilistic graphical model for the classification of mobile LiDAR point clouds. *ISPRS Journal of*

- Photogrammetry and Remote Sensing, 143, 108–123. https://doi.org/10.1016/j.isprsjprs.2018.04.018
- Lai, X., Yuan, Y., Li, Y., & Wang, M. (2019). Full-waveform LiDAR point clouds classification based on wavelet support vector machine and ensemble learning. Sensors, 19(14), Article 3191. https://doi.org/10.3390/s19143191
- Li, W., Wang, F. D., & Xia, G. S. (2020). A geometry-attentional network for ALS point cloud classification. *ISPRS Journal of Photogrammetry and Remote Sensing*, 164, 26–40. https://doi.org/10.1016/j.isprsjprs.2020.03.016
- Lin, Y., Wang, C., Zhai, D., Li, W., & Li, J. (2018). Toward better boundary preserved supervoxel segmentation for 3D point clouds. *ISPRS Journal of Photogrammetry and Remote Sensing*, 143, 39–47. https://doi.org/10.1016/j.isprsjprs.2018.05.004
- Lu, Q., Chen, C., Xie, W., & Luo, Y. (2020). PointNGCNN: Deep convolutional networks on 3D point clouds with neighborhood graph filters. *Computers & Graphics*, 86, 42–51. https://doi.org/10.1016/j.cag.2019.11.005
- Park, Y., & Guldmann, J.-M. (2019). Creating 3D city models with building footprints and LIDAR point cloud classification: A machine learning approach. *Computers, Environment and Urban Systems*, 75, 76–89.
  - https://doi.org/10.1016/j.compenvurbsys.2019.01.004
- Peyghambarzadeh, S. M. M., Azizmalayeri, F., Khotanlou, H., & Salarpour, A. (2020). Point-PlaneNet: Plane kernel based convolutional neural network for point clouds analysis. *Digital Signal Processing: A Review Journal*, 98, Article 102633. https://doi.org/10.1016/j.dsp.2019.102633
- Pujol-Miró, A., Casas, J. R., & Ruiz-Hidalgo, J. (2019). Correspondence matching in unorganized 3D point clouds using convolutional neural networks. *Image and Vision Computing*, 83–84, 51–60. https://doi.org/10.1016/j.imavis.2019.02.013
- Rastiveis, H., Shams, A., Sarasua, W. A., & Li, J. (2020). Automated Extraction of Lane Markings from Mobile LiDAR Point Clouds Based on Fuzzy Inference. *ISPRS Journal of Photogrammetry and Remote Sensing*, *160*, 149–166. https://doi.org/10.1016/j.isprsjprs.2019.12.009
- Stojanovic, V., Trapp, M., Richter, R., & Döllner, J. (2019). Service-oriented semantic enrichment of indoor point clouds using octree-based multiview classification. *Graphical Models*, 105, Article 101039. https://doi.org/10.1016/j.gmod.2019.101039
- Suomalainen, J., Hakala, T., Kaartinen, H., Räikkönen, E., & Kaasalainen, S. (2011). Demonstration of a virtual active hyperspectral LiDAR in automated point cloud classification. *ISPRS Journal of Photogrammetry and Remote Sensing*, *66*(5), 637–641. https://doi.org/10.1016/j.isprsjprs.2011.04.002
- Tseng, Y. H., Wang, C. K., Chu, H. J., & Hung, Y. C. (2015). Waveform-based point cloud classification in land-cover identification. *International Journal of Applied Earth Observation and Geoinformation*, 34(1), 78–88. https://doi.org/10.1016/j.jag.2014.07.004
- Weidner, L., Walton, G., & Kromer, R. (2019). Classification methods for point clouds in rock slope monitoring: A novel machine learning approach and comparative analysis. *Engineering Geology*, 263, Article 105326. https://doi.org/10.1016/j.enggeo.2019.105326
- Weidner, L., Walton, G., & Kromer, R. (2020). Generalization considerations and solutions for point cloud hillslope classifiers. Geomorphology, 354, Article 107039. https://doi.org/10.1016/j.geomorph.2020.107039
- Wen, C., Sun, X., Li, J., Wang, C., Guo, Y., & Habib, A. (2019). A deep learning framework for road marking extraction, classification and completion from mobile laser scanning point clouds. *ISPRS Journal of Photogrammetry and Remote Sensing*, 147, 178–192. https://doi.org/10.1016/j.isprsjprs.2018.10.007

Wen, C., Yang, L., Li, X., Peng, L., & Chi, T. (2020). Directionally constrained fully convolutional neural network for airborne LiDAR point cloud classification. *ISPRS Journal of Photogrammetry and Remote Sensing*, 162, 50–62.

#### https://doi.org/10.1016/j.isprsjprs.2020.02.004

Williams, R. M., & Ilieş, H. T. (2018). Practical shape analysis and segmentation methods for point cloud models. *Computer Aided Geometric Design*, 67, 97–120.

### https://doi.org/10.1016/j.cagd.2018.10.003

- Xue, F., Lu, W., Webster, C. J., & Chen, K. (2019). A derivative-free optimization-based approach for detecting architectural symmetries from 3D point clouds. ISPRS Journal of Photogrammetry and Remote Sensing, 148, 32–40.
  - https://doi.org/10.1016/j.isprsjprs.2018.12.005
- Yang, Y., Chen, F., Wu, F., Zeng, D., Ji, Y., & Jing, X.-Y. (2020a). Multi-view semantic learning network for point cloud based 3D object detection. *Neurocomputing*, 397, 477–485. https://doi.org/10.1016/j.neucom.2019.10.116
- Yang, Y., Fang, H., Fang, Y., & Shi, S. (2020b). Three-dimensional point cloud data subtle feature extraction algorithm for laser scanning measurement of large-scale irregular surface in reverse engineering. *Measurement: Journal of the International Measurement Confederation*, 151, Article 107220. https://doi.org/10.1016/j.measurement.2019.107220
- Zhu, Q., Li, Y., Hu, H., & Wu, B. (2017). Robust point cloud classification based on multi-level semantic relationships for urban scenes. ISPRS Journal of Photogrammetry and Remote Sensing, 129, 86–102. https://doi.org/10.1016/j.isprsjprs.2017.04.022